Cu XAS Shows a Change in the Ligation of Cu_B upon Reduction of Cytochrome bo_3 from *Escherichia coli*†

Jeffrey P. Osborne,‡ Nathaniel J. Cosper,§ Christina M. V. Stålhandske,§ Robert A. Scott,§ James O. Alben,|| and Robert B. Gennis*,‡

Department of Biochemistry, University of Illinois, Urbana, Illinois 61801, Department of Chemistry, The University of Georgia, Athens, Georgia 30602, and Department of Medical Biochemistry, The Ohio State University, Columbus, Ohio 43210

Received September 22, 1998; Revised Manuscript Received January 26, 1999

ABSTRACT: Copper X-ray absorption spectroscopy (XAS) has been used to examine the structures of the Cu(II) and Cu(I) forms of the cytochrome bo_3 quinol oxidase from *Escherichia coli*. Cytochrome bo_3 is a member of the superfamily of heme−copper respiratory oxidases. Of particular interest is the fact that these enzymes function as redox-linked proton pumps, resulting in the net translocation of one H^+ per electron across the membrane. The molecular mechanism of how this pump operates and the manner by which it is linked to the oxygen chemistry at the active site of the enzyme are unknown. Several proposals have featured changes in the coordination of Cu_B during enzyme turnover that would result in sequential protonation or deprotonation events that are key to the functioning proton pump. This would imply lability of the ligands to Cu_B. In this work, the structure of the protein in the immediate vicinity of Cu_B, in both the fully oxidized and fully reduced forms of the enzyme, has been examined by Cu XAS, a technique that is particularly sensitive to changes in metal coordination. The results show that in the oxidized enzyme, Cu_B(II) is four-coordinate, consistent with three imidazoles and one hydroxyl (or water). Upon reduction of the enzyme, the coordination of Cu_B(I) is significantly altered, consistent with the loss of one of the histidine imidazole ligands in at least a substantial fraction of the population. These data add to the credibility that changes in the ligation of Cu_B might occur during catalytic turnover of the enzyme and, therefore, could, in principle, be part of the mechanism of proton pumping.

The heme−copper oxidases are critical components of the respiratory chains of virtually all eukaryotes as well as aerobic prokaryotes (*1*−*3*). This superfamily of enzymes includes both cytochrome *c* oxidases and quinol oxidases, such as cytochrome bo_3 from *Escherichia coli.* These enzymes all catalyze the four-electron reduction of dioxygen to water, and utilize the considerable free energy made available from this reaction to generate a transmembrane proton-motive force. A portion of this proton-motive force results from the coupling of the redox chemistry catalyzed by the enzyme to a transmembrane electrogenic proton pump. For each dioxygen reduced to water ($4e^- + 4H^+ + O_2 \leftrightarrow 2H_2O$), four protons are pumped across the membrane electrogenically ($4H^+_{in} \leftrightarrow 4H^+_{out}$). The X-ray structures of the cytochrome *c* oxidases from *Paracoccus denitrificans* (*4*, *5*) and from bovine heart mitochondria (*6*−*8*) have provided an essential guide for designing and interpreting experiments related to the dynamics of the proton pump, but do not provide a clear answer for how this pump works. Several putative proton-conducting channels are perceived within the structures of the oxidases (all within subunit I) (*4*, *5*, *7*, *8*), and several residues within these channels have been demonstrated to be functionally important on the basis of site-directed mutagenesis studies (*9*, *10*). Such channels must be important for providing pathways both for protons consumed in the chemistry at the heme−copper active site of the enzyme and also for protons that are pumped across the membrane. It should be noted that no high-resolution structure has been reported for any of the quinol oxidases (such as cytochrome bo_3); however, there is considerable amino acid sequence homology, and these quinol oxidases are generally thought to function like the cytochrome *c* oxidases in the heme−copper oxidase superfamily.

There is considerable evidence (*9*, *10*) from site-directed mutagenesis of the bacterial heme−copper oxidases, including the cytochrome bo_3 quinol oxidase from *E. coli*, that all of the pumped protons use the D-channel on the input side of the enzyme (bacterial cytoplasm). This leads from D135 (*E. coli* numbering; corresponding to D91 in the bovine oxidase) near the surface of the protein to E286 (corresponding to E242 in the bovine oxidase) which is about 25 Å away. It has been suggested that several water molecules, not observed in the structures, but present transiently, may provide a proton-wire connection to the heme−copper active site (*11*), where protons could be used in the water-generating

† Supported by a grant from the Department of Energy (DEFG02-87ER13716 to R.B.G.) and by the National Institutes of Health (NIH) (Grant GM 42025 to R.A.S.). The XAS data were collected at the Stanford Synchrotron Radiation Laboratory (SSRL), which is operated by the Department of Energy, Division of Chemical Sciences. The SSRL Biotechnology Program is supported by the NIH, Biomedical Resource Technology Program, Division of Research Resources. N.J.C. is supported by a National Science Foundation Research Training Group Award to the Center for Metalloenzyme Studies (DIR 90-14281).

* To whom correspondence should be addressed. Telephone: (217) 333-9075. Fax: (217) 244-3186. E-mail: r-gennis@uiuc.edu.

‡ University of Illinois.

§ The University of Georgia.

|| The Ohio State University.

10.1021/bi982278y CCC: $18.00
Published on Web 03/16/1999

chemistry or directed across the membrane as pumped protons. FTIR spectroscopy does detect conformational changes at E286 in cytochrome bo_3 that appear to be induced by CO interacting with Cu_B (*12*) or by reduction of the metals (*13*, *14*). Changes in the coordination of Cu_B have been explicitly proposed as a plausible mechanism for driving the pumping machinery (*5*, *15*), consistent with utilization of this input pathway. It has also been proposed, though without any detailed coupling mechanisms, that (1) the pumped protons are directed by the E286 shuttle to an exit route that does not pass directly through the heme−copper center but, rather, via proposed water molecules to a heme propionate group in the exit pathway (*16*) or (2) the pumped protons do not utilize the D-channel, but a different route referred to as the H-channel, which is distant from the heme−copper active site (*8*). Clearly, further experimental data are needed to distinguish the possibilities.

The fundamental question addressed in the current work is whether the coordination of Cu_B might change during turnover of the enzyme. The first experiment involves simply asking whether changes in the redox state of the metals result in significant changes in the coordination of Cu_B. X-ray absorption spectroscopy (*17*−*22*) provides a sensitive tool for evaluating the structure of the protein within about 4 Å of the copper atom, and is partucularly useful since the structures of both the bovine and *Paracoccus* cytochrome *c* oxidases have been determined (*4*, *5*, *7*, *8*). In both cases, the fully oxidized enzymes have been shown to have three histidine imidazoles ligated to Cu_B (*4*, *8*), which provides a firm basis for modeling XAS results. The data from X-ray diffraction studies of the bovine enzyme (about 2.35 Å resolution) indicate that the structure of the protein in the immediate vicinity of the heme−copper center does not change upon full reduction of the metals (*8*). However, in the oxidized enzyme, the data are interpreted to indicate a peroxide molecule ligated end-on to Cu_B, whereas no nonprotein ligand is apparent in the fully reduced enzyme (*8*). The structure of the oxidized two-subunit form of the *Paracoccus* cytochrome *c* oxidase indicates bridging electron density between the heme a_3 Fe and Cu_B, which cannot be deciphered (at 2.7 Å resolution), but would be consistent with Cu_B hydroxide with a water on or near the Fe (*4*). However, it has also been shown that when the four-subunit form of the oxidized *Paracoccus* cytochrome *c* oxidase is cocrystallized with azide, one of the three histidine imidazole ligands to Cu_B is apparently displaced (*5*). The important implication is that the coordination of Cu_B is labile and suggests that it is reasonable to postulate such coordination changes in the different redox states and oxygenated intermediates generated during catalytic turnover.

The XAS data in the current work show that reduction of the cytochrome bo_3 quinol oxidase results in a definite change in the coordination of Cu_B, consistent with the loss of one of the three histidine imidazole ligands. The XAS data obtained with the oxidized form of the quinol oxidase are consistent with the presumed structure in the vicinity of Cu_B based on the X-ray structures of the two cytochrome *c* oxidases. However, the XAS data are not consistent with the reported X-ray structure of the reduced bovine cytochrome *c* oxidase (*8*), possibly reflecting a difference between the two heme−copper oxidases, i.e., the bovine cytochrome *c* oxidase and the bacterial quinol oxidase.

MATERIALS AND METHODS

Cell Growth. At the University of Illinois fermentation facility, phage free cells from *E. coli* strain GO105/pJRHisA (*23*), freshly grown on an LB plate containing 100 μg/mL ampicillin and 50 μg/mL kanamycin, were used to inoculate four 10 mL cultures which were grown during the course of a day. These cultures were used to inoculate four 300 mL cultures. After growing to an OD of 0.1, these cultures were used to inoculate a 200 L fermentor containing 2080 g of K_2HPO_4, 600 g of KH_2PO_4, 150 g of sodium citrate, 500 g of $(NH_4)_2SO_4$, 2000 g of tryptone, 1000 g of yeast extract, 1000 g of casamino acids, 4 L of glycerol, 20 g of L-tryptophan, 20 g of $MgSO_4$, 10 g of $FeSO_4$, 5 g of $CuSO_4$, 20 g of ampicillin, and 10 g of kanamycin (*24*) as well as 2 mL of Antifoam (Sigma). The fermentor conditions were 37 °C, 20 psi backpressure, 300 mbar air pressure, $^1/_2$ volume air per minute sparging up from the bottom, and 300 rpm. Cells were harvested before the stationary phase after about 6 h and were dark red.

Protein Purification. Cytochrome bo_3 was purified as described previously (*23*), with the following exceptions. Cells were broken by passing 10 times through a microfluidizer (Microfluidics Corp., Newton, MA). The soluble protease inhibitor 4-(2-aminoethyl)benzenesulfonyl fluoride (AEBSF) was added to a concentration of approximately 1 mM before using the microfluidizer, and phenylmethanesulfonyl fluoride (PMSF) was added afterward. Membranes were pelleted by ultracentrifugation at 125000*g* for 4 h. The only detergent used in the purification was *n*-dodecyl β-D-maltoside, which was used at concentrations of 1 wt %/vol for solubilization and 0.1% for running the column. The final dialysis was against either 0.02 or 0.1% *n*-dodecyl β-D-maltoside, 100 mM HEPES, and 1 mM EDTA (pH 7.4). The protein was concentrated to at least 80 μM, transferred to screwtop cryovials, flash-frozen in liquid nitrogen, and stored at −80 °C until it was used.

The as-isolated cytochrome bo_3 exhibited a Soret peak at 408 nm, indicative of a "fast" preparation (*25*). The cytochrome bo_3 concentration was based on an ϵ_{408nm} of 188 mM^{-1} cm^{-1} for the oxidized enzyme. This extinction coefficient is similar to a value (ϵ_{408nm} = 183 mM^{-1} cm^{-1}) described previously (*26*) but determined independently. Quinone and heme analyses were performed as described previously (*23*). UQ_8 was present at a ratio of about 1.5 per enzyme, and heme analysis revealed that equal amounts of hemes B and O were present. Activity assays were carried out by monitoring the decrease in the concentration of oxygen with a Clark oxygen electrode (Yellow Springs Instrument Co., Yellow Springs, OH). Assay conditions were 50 mM sodium phosphate, 5 mM EDTA (pH 7.5), and 20 mM dithiothreitol at 37 °C. Protein was added and a baseline recorded. UQ_1 was added to a final concentration of 245 μM to start the reaction. With the assumption that the concentration of O_2 in the solution before protein addition was 237 μM, the protein exhibited a turnover of at least 590 electrons s^{-1} cyt bo_3^{-1}, indicating that the enzyme is fully active. It is noted that the preparations of enzyme used for these experiments are free from halides such as chloride.

XAS Sample Preparation. The protein was concentrated using Centriprep-100 (Amicon) or Ultrafree 50 kDa cutoff (Millipore) centrifuge concentrators. Increasing the temper-

ature of the centrifuge to 14 °C increased the rate and extent of concentration, presumeably by lowering the sample viscosity. Glycerol was added to the protein while it was being stirred to a final concentration of 30% v/v.

Oxidized samples were used as-purified and transferred directly into the XAS cuvettes.

For the reduced samples, the protein was placed, along with a magnetic stirring flea, in 3 mL screwtop reaction vials. Sufficient 1 M ascorbate was added onto the inside wall of the vial to effect a final concentration of either 10 or 90 mM in independent samples. The ascorbate used was at either pH 8 or 9, depending on the sample, resulting in a final pH between approximately 7.5 and 8.0. Additionally, enough 32 mM phenazine methosulfate (PMS) was added to the wall to make the concentration approximately 16 μM. The cap containing a Teflon/silicon insert was screwed on tightly with the silicon side in, and the headspace above the protein in the vial was replaced by N_2 introduced through needles spanning the Teflon/silicon insert. The needles were removed, leaving a positive nitrogen gas pressure in the vial, and the vial was spun in a clinical centrifuge for 30 s to transfer the reductants from the side of the vial into the protein solution. Mixing was completed with a magnetic stirrer and manual swirling. Subsequently, the sample was collected in the bottom of the vial by another 30 s spin in a clinical centrifuge. The sample was left at room temperature for 3 h for reduction. The reaction vial was transferred to a nitrogen atmosphere in a model R-17-17H glovebag (Instruments for Reasearch and Industry, Cheltenham, PA) that had been made anaerobic by filling and purging with nitrogen gas and was maintained under a positive nitrogen gas pressure. In the glovebag, the XAS cuvette was purged with nitrogen gas and then filled with the sample using a syring and needle. After the XAS cuvette was capped, the sample was allowed to stand for 5 min so that the small bubbles in the sample rose to the top, leaving an optically clear sample. During this time, the protein reduced any oxygen that it happend to contact during the transfer to the cuvette and ultimately became fully reduced. The color change upon reduction was visually apparent.

Samples were dropped horizontally into a Styrofoam cup containing a few millimeters of liquid nitrogen for rapid freezing. Samples were then frozen in polycarbonate cuvettes (24 mm × 3 mm × 1 mm) with a 0.025 mm Mylar window covering one 24 mm × 3 mm face. The samples were stored at or below −57 °C until data acquisition was carried out.

XAS. XAS data were collected at Stanford Synchrotron Radiation Laboratory (SSRL) with the SPEAR storage ring operating in a dedicated mode at 3.0 GeV (Table 1). Analysis was performed on the average of three data sets for the reduced enzyme, and two data sets for the oxidized enzyme, each collected on separately prepared samples. EXAFS analysis was performed with the EXAFSPAK software (courtesy of G. N. George; http://ssrl01.slac.stanford.edu/exafspak.html) according to standard procedures (*19*). Both single- and multiple-scattering paths ≤4.5 Å from the Cu atom were used to identify and quantify imidazole coordination due to histidine. Multiple-scattering paths were built by importing the crystal structure of tetrakis(imidazole)copper(II) sulfate (*27*) into Ball & Stick software (version 3.5, Cherwell Scientific). The model was edited to only the copper atom and one imidazole, and the coordinates were imported into FEFF version 5.05 (*28*) to calculate scattering amplitudes and phase shifts for each scattering path containing four or fewer legs. A constrained fitting process was then used with the following parameters. Coordination numbers were constrained to integer or half-integer (implying a mixture of species) values; the distances for outer-shell atoms of imidazole rings were constrained to a constant difference with the first-shell (metal−nitrogen or −oxygen) distance. Only a single ΔE_0 value was optimized. Debye−Waller values for the outer-shell atoms of imidazole rings were constrained to be a multiple of the first-shell value. The bond valence sum (BVS) method was applied to EXAFS-simulated coordination environments using standard procedures (*29*−*31*). Possible coordination numbers of histidyl imidazole ligands were chosen from fits that yielded chemically and physically reasonable Debye−Waller factors for the outer-shell atoms. In Cu imidazole model compounds, we find that the following Debye−Waller factors are typical: Cu−N_1, $\sigma_{as}^2 = 0.001-0.003$ Å^2; Cu···(C_2, C_5), $\sigma_{as}^2 = 0.002-0.004$ Å^2; and Cu···(N_3, C_4), $\sigma_{as}^2 = 0.003-0.006$ Å^2.

Table 1: X-ray Absorption Spectroscopic Data for Cu Cyt bo_3 Samples[a]

	Cu EXAFS
SR facility	SSRL
beamline	7−3
current in storage ring (mA)	55−85
monochromator crystal	Si[220]
detection method	fluorescence
detector type	solid state array
scan length (min)	26
no. of scans in average	10
temperature (K)	10
energy standard	Cu foil, first inflection
energy calibration (eV)	8980.3
E_0 (eV)	8990
pre-edge background	
energy range (eV)	8657−8945
Gaussian center (eV)	8040
width (eV)	750
spline background	
energy range (eV) (polynomial order)	8990−9208 (4)
	9208−9427 (4)
	9427−9646 (4)

[a] The 13-element Ge solid state X-ray fluorescence detector at SSRL is provided by the NIH Biotechnology Research Resource.

RESULTS

Edge Spectra. The Cu K-edge X-ray absorption spectra for oxidized and reduced cytochrome bo_3 show the expected shift between Cu(II) and Cu(I), respectively (*32*). Hence, it is certain that the oxidase is reduced and oxidized, respectively, in the two samples being compared. The edge for Cu(I) cytochrome bo_3 (Figure 1) shows a pre-edge peak at 8983 eV which is assigned as a 1s4p transition (plus shakedown) (*32*). The normalized peak intensity of 0.372, along with the peak position (*32*), indicates a coordination number of 3 for Cu(I) in cytochrome bo_3.

EXAFS. EXAFS data for both Cu(I) and Cu(II) cytochrome bo_3 display adequate signal-to-noise ratios to a k of 12 Å^{-1} (Figures 2 and 3). The Cu(II) data (Figure 2) are best fit assuming a coordination number of 4, which also yields reasonable BVS (bond valence sum) values (*29*−*31*) (Table 2; more detailed fit information is provided in Table S1 of

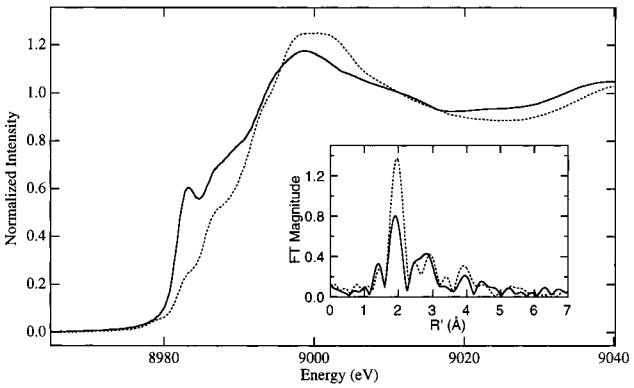

FIGURE 1: Cu X-ray absorption edge spectra of Cu(II) (···) and Cu(I) cytochrome bo_3 (—). In the inset, the Fourier transforms of Cu EXAFS for Cu(II) (···) and Cu(I) cytochrome bo_3 (—) are compared.

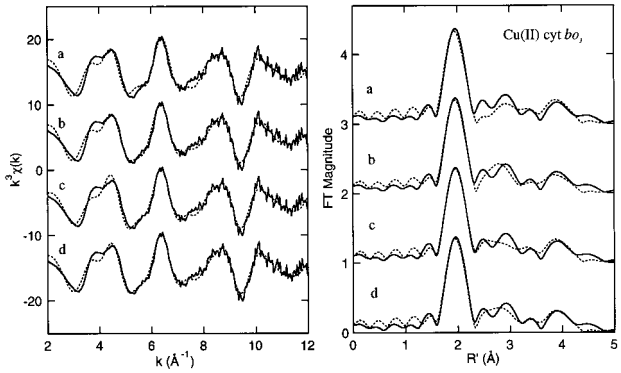

FIGURE 2: k^3-weighted Cu EXAFS (left) and Fourier transform (right; over the k range of 2−12 Å^{-1}) of Cu(II) cyt bo_3 (—) compared with fits of (a) $Cu(N/O)_1(imid)_3$ (Table 2, fit 1), (b) $Cu(N/O)_1(imid)_3S$ (Table 2, fit 2), (c) $Cu(N/O)_1(imid)_3(N/O)_2$ (Table 2, fit 4), and (d) $Cu(N/O)_1(imid)_3Fe$ (Table 2, fit 5).

the Supporting Information). The Fourier transform (FT) peaks at 3 and 4 Å are best fit assuming the presence of the outer-shell atoms of three histidine imidazole ligands. The fourth ligand is reasonably assigned as hydroxide. The Debye−Waller factor values resulting from three-imidazole fits are larger than expected for a well-ordered set of imidazole ligands. Ascribing the increased Debye−Waller factor values to static disorder would require Cu−N(imid) distances that differ by 0.10−0.14 Å (ΔR_{as}[1]).

A small maximum appears at 2.5 Å in the FT of the Cu(II) EXAFS (Figure 2), and this feature is present and relatively more significant in the Cu(I) FT (vide infra) (Figure 3). This peak at 2.5 Å in the Cu(II) data can be fit by an Fe (or another first-row transition metal) or by one or two O or N atoms (Table 2, fits 3−5). Fitting the shell with a S or Cl atom results in a much higher Debye−Waller factor for imidazole atoms (Table 2, fit 2) than similar fits with Fe, or O or N, atoms (Table 2, fits 3−5). Fits including this shell (Fe, O or N, or S or Cl) result in an improvement in the goodness-of-fit value of approximately 10% (Table 2, fits

[1] ΔR_{as} is estimated with the equation $\sigma_{stat} \approx (mn)^{1/2}/(m+n)|R_m - R_n|$, where $\sigma_{stat} = (\sigma_{as}^2 - \sigma_{vib}^2)^{1/2}$ and m and n are the number of atoms at a distance of R_m and R_n, respectively. With $m = 2$ and $n = 1$, and an estimated σ_{vib}^2 of 0.004 Å^2 for the ~3 Å shell, an observed σ_{as}^2 of 0.0062 Å^2 would require $|R_m - R_n|$ to be 0.10 Å. An estimated σ_{vib}^2 of 0.002 Å^2 with an observed σ_{as}^2 of 0.0062 Å^2 would require $|R_m - R_n|$ to be 0.14 Å.

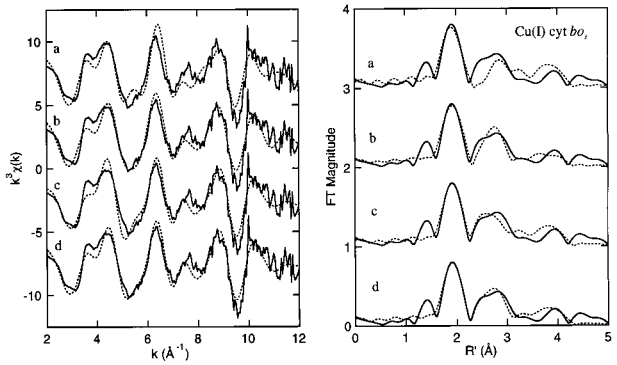

FIGURE 3: k^3-weighted Cu EXAFS (left) and Fourier transform (right; over the k range of 2−12 Å^{-1}) of Cu(I) cyt bo_3 (—) compared with fits of (a) $Cu(N/O)_{0.5}(imid)_{2.5}$ (Table 3, fit 1), (b) $Cu(N/O)_{0.5}(imid)_{2.5}S$ (Table 3, fit 2), (c) $Cu(N/O)_{0.5}(imid)_{2.5}(N/O)_2$ (Table 3, fit 4), and (d) $Cu(N/O)_{0.5}(imid)_{2.5}Fe$ (Table 3, fit 5).

2−5) compared to a similar fit without this shell (Table 2, fit 1). Minor improvements in the match of simulated EXAFS and FT with the observed data with Cu(II) result from inclusion of this additional shell (Figure 2). Inclusion of one O or N atom at 2.5 Å results in a reasonable Debye−Waller factor for that shell (Table 2, fit 3), whereas a fit with two O or N atoms results in a Debye−Waller factor that requires significant disorder in those atoms[2] (Table 2, fit 4). The Cu(II) data are most reasonably interpreted as being due to a single solvent (water) molecule located about 2.5 Å from Cu_B in the oxidized enzyme, in addition to the three histidine imidazoles and hydroxide that are coordinated to Cu_B.

The Cu(I) data are best fit assuming a coordination number of 3, which yields reasonable BVS values (Table 3; more detailed fit information is given in Table S2 of the Supporting Information), and agrees with analysis of the edge region. The peaks at 3 and 4 Å in the FT can be fit by either 2 or 2.5 histidine imidazole ligands; i.e., half of the enzyme is coordinated to 2 and half is coordinated to 3 histidine imidazoles. However, the fit with 2.5 imidazoles results in outer-shell imidazole atom Debye−Waller factors that are most similar to those observed for the three-imidazole fits of the Cu(II) cytochrome bo_3 data (cf., fit 5 in Tables 2 and 3). The data, thus, are interpreted to indicate coordination of Cu_B in the reduced oxidase to two histidine imidazoles and water. One of the histidine imidazoles coordinated to Cu_B in the oxidized enzyme has moved away from the metal in a substantial fraction of the population.

As observed with the Cu(II) form of the quinol oxidase (Figure 2), the FT of the data obtained with the reduced enzyme also shows a peak at 2.5 Å (Figure 3). This can also be fit by an Fe or by one or two O or N atoms (Table 3, fits 3−5), resulting in an approximately 15% improvement in the goodness-of-fit value compared to that for a similar fit without this shell (Table 3, fit 1). Again, simulations based on a S or Cl atom in the additional shell result in increased imidazole atom Debye−Waller factors (Table 3, fit 2) compared with fits with one Fe or two O or N atoms (Table 3, fits 4 and 5). Hence, a S or Cl atom is disfavored. Simulations based on one O or N (Table 3, fit 3) result in unreasonably low Debye−Waller factors, whereas those

[2] As in footnote 1, an observed σ_{as}^2 of 0.0101 Å^2 (with $m = n = 1$) would require $|R_m - R_n|$ to be 0.16−0.18 Å.

Table 2: Curve Fitting Results for Cu EXAFS Modeled as $Cu(imid)_x(N,O)_y(S/Cl,Fe,O)_z$[a]

sample file name (*k* range)	fit	*x*, *y*, *z*	shell	N_s	R_{as} (Å)	σ_{as}^2 (Å^2)[b]	ΔE_0 (eV)[b]	*f*′[c]	BVS[d]
Cu(II) cytochrome bo_3 COOXBC (2−12)	1	3, 1, 0	Cu−N or −O	4	1.95	0.0040	−0.60	0.072	2.34
			Cu−C	3	2.95	0.0040	[−0.60]		
			Cu−C	3	2.98	[0.0040]	[−0.60]		
			Cu−C	3	4.12	[0.0056]	[−0.60]		
			Cu−N	3	4.10	[0.0056]	[−0.60]		
	2	3, 1, 1	Cu−N or −O	4	1.95	0.0042	−0.55	0.067	2.34
			Cu−C	3	2.95	0.0070	[−0.55]		
			Cu−C	3	2.98	[0.0070]	[−0.55]		
			Cu−C	3	4.12	[0.0098]	[−0.55]		
			Cu−N	3	4.10	[0.0097]	[−0.55]		
			Cu−S or −Cl	1	2.74	0.0050	[−0.55]		
	3	3, 1, 1	Cu−N or −O	4	1.93	0.0042	−0.53	0.066	2.47
			Cu−C	3	2.92	0.0045	[−0.53]		
			Cu−C	3	2.94	[0.0045]	[−0.53]		
			Cu−C	3	4.08	[0.0062]	[−0.53]		
			Cu−N	3	4.06	[0.0062]	[−0.53]		
			Cu−N or −O	1	2.56	0.0032	[−0.53]		
	4	3, 1, 2	Cu−N or −O	4	1.95	0.0042	−0.59	0.068	2.34
			Cu−C	3	2.94	0.0042	[−0.59]		
			Cu−C	3	2.97	[0.0042]	[−0.59]		
			Cu−C	3	4.11	[0.0059]	[−0.59]		
			Cu−N	3	4.10	[0.0059]	[−0.59]		
			Cu−N or −O	2	2.55	0.0101	[−0.59]		
	5	3, 1, 1	Cu−N or −O	4	1.95	0.0041	−0.23	0.066	2.34
			Cu−C	3	2.95	0.0053	[−0.23]		
			Cu−C	3	2.98	[0.0053]	[−0.23]		
			Cu−C	3	4.12	[0.0074]	[−0.23]		
			Cu−N	3	4.11	[0.0074]	[−0.23]		
			Cu−Fe	1	2.59	0.0116	[−0.23]		

[a] Group is the chemical unit defined for the multiple-scattering calculation. N_s is the number of scatterers (or groups) per metal. R_{as} is the metal−scatterer distance. σ_{as}^2 is the mean-square deviation in R_{as}. ΔE_0 is the shift in E_0 for the theoretical scattering functions. [b] Numbers in square brackets were constrained either to be a multiple of the above value (σ_{as}^2) or to maintain a constant difference from the above value (R_{as} or ΔE_0). [c] f' is a normalized error (χ^2); $f' = \{\Sigma_i[k^3(\chi_i^{obs} - \chi_i^{calc})]^2/N\}^{1/2}/[(k^3\chi^{obs})_{max} - (k^3\chi^{obs})_{min}]$. [d] BVS = Σs. $s = \exp[(r_0 - r)/B]$, where $B = 0.37$, r_0[Cu(II)−N] = 1.769, and $r0$[Cu(I)−N] = 1.595 (*31*).

based on two O or N or one Fe result in more reasonable values (Table 3, fits 4 and 5). The most reasonable interpretation is that there are two O or N atoms located approximately 2.5 Å from Cu_B in the reduced enzyme in addition to the coordination provided by two histidine imidazoles and by one water. One of the 2.5 Å O or N atoms can be accounted for by a second solvent molecule in the region between the heme Fe and Cu_B. The second 2.5 Å O or N atom can be due to the imidazole nitrogen that has moved out of the coordination sphere; i.e., it has shifted from being 1.93 Å to being about 2.5 Å from Cu_B.

DISCUSSION

The main conclusion from this work is that there is a change in the protein structure in the immediate vicinity of Cu_B upon reduction of the cytochrome bo_3 quinol oxidase. This quinol oxidase provides an excellent system for Cu XAS since Cu_B is the only copper present in the enzyme. It is not feasible to use this approach to examine the cytochrome *c* oxidases, such as the two for which X-ray structures are known, from *Paracoccus* or from bovine heart mitochondria, since in these enzymes two additional copper atoms are present in the form of the binuclear Cu_A redox center. Cu_A is absent in the quinol oxidases, so the X-ray absorption of Cu_B can be examined without interference. This was previously taken advantage of in a study of the EXAFS of the aa_3-type quinol oxidase from *Bacillus subtilis* (*18*). It was concluded that Cu_B in the oxidized form of the *Bacillus* quinol oxidase was coordinated to three histidine imidazoles and hydroxide (or water). The data presented in the current study of the oxidized *E. coli* quinol oxidase support the same conclusion that Cu_B is four-coordinate, with three histidine imidazoles and one hydroxide. It is also assured from the XAS data for cytochrome bo_3 that the copper is in the Cu(II) state in the sample of oxidized enzyme and has not been reduced by the X-ray beam.

The very strong sequence homologies (*1*) suggest that the quinol oxidases (*Bacillus* aa_3 or *E. coli* bo_3) in the vicinity of the heme−copper binuclear center should have virtually the same structure as observed in the X-ray structures of the cytochrome *c* oxidases. Most of the amino acids located within 10 Å of Cu_B are conserved in cytochrome bo_3, and it is unlikely that these differences will influence the immediate vicinity of Cu_B. For example, glycine-319 in the *Paracoccus* cytochrome *c* oxidase is replaced by a serine (S327) in the cytochrome bo_3 quinol oxidase. The α-carbon of the glycine (G319) in the *Paracoccus* oxidase is 7.7 Å from Cu_B, and it seems unlikely that this substitution in the *E. coli* oxidase will have any direct effect on Cu_B. The X-ray structure of the oxidized two-subunit *Paracoccus* cytochrome *c* oxidase (*4*) is consistent with the contention that the quinol oxidases and cytochrome *c* oxidases have essentially the same structures, indicating three histidine imidazoles for certain, and the likelihood of an additional hydroxide (or water) on Cu_B.

Similarly, the higher-resolution structure of the eukaryotic bovine heart cytochrome *c* oxidase also shows three histidine imidazole ligands (*8*). However, the X-ray structure of the "oxidized" bovine cytochrome *c* oxidase has been interpreted as containing a peroxide molecule ligated end-on to Cu_B,

Table 3: Curve Fitting Results for Cu EXAFS Modeled as $Cu(imid)_x(N,O)_y(S/Cl,Fe,O)_z$[a]

sample file name (*k* range)	fit	*x, y, z*	shell	N_s	R_{as} (Å)	σ_{as}^2 (Å^2)[b]	ΔE_0 (eV)[b]	f'[c]	BVS[d]
Cu(I) cytochrome bo_3 CORDBCD (2−12)	1	2.5, 0.5, 0	Cu−N or −O	3	1.93	0.0068	−3.47	0.121	1.21
			Cu−C	2.5	2.91	0.0030	[−3.47]		
			Cu−C	2.5	2.95	[0.0030]	[−3.47]		
			Cu−C	2.5	4.07	[0.0042]	[−3.47]		
			Cu−N	2.5	4.06	[0.0042]	[−3.47]		
	2	2.5 ,0.5, 1	Cu−N or −O	3	1.93	0.0067	−3.40	0.102	1.21
			Cu−C	2.5	2.91	0.0098	[−3.40]		
			Cu−C	2.5	2.94	[0.0098]	[−3.40]		
			Cu−C	2.5	4.07	[0.0138]	[−3.40]		
			Cu−N	2.5	4.06	[0.0138]	[−3.40]		
			Cu−S or −Cl	1	2.72	0.0027	[−3.40]		
	3	2.5, 0.5, 1	Cu−N or −O	3	1.93	0.0069	−3.57	0.099	1.21
			Cu−C	2.5	2.91	0.0040	[−3.57]		
			Cu−C	2.5	2.94	[0.0040]	[−3.57]		
			Cu−C	2.5	4.07	[0.0055]	[−3.57]		
			Cu−N	2.5	4.06	[0.0055]	[−3.57]		
			Cu−N or −O	1	2.53	0.0006	[−3.57]		
	4	2.5, 0.5, 2	Cu−N or −O	3	1.92	0.0068	−3.94	0.102	1.25
			Cu−C	2.5	2.91	0.0040	[−3.94]		
			Cu−C	2.5	2.94	[0.0040]	[−3.94]		
			Cu−C	2.5	4.07	[0.0056]	[−3.94]		
			Cu−N	2.5	4.06	[0.0056]	[−3.94]		
			Cu−N or −O	2	2.53	0.0053	[−3.94]		
	5	2.5, 0.5, 1	Cu−N or −O	3	1.93	0.0066	−2.98	0.096	1.21
			Cu−C	2.5	2.91	0.0056	[−2.98]		
			Cu−C	2.5	2.94	[0.0056]	[−2.98]		
			Cu−C	2.5	4.07	[0.0077]	[−2.98]		
			Cu−N	2.5	4.06	[0.0078]	[−2.98]		
			Cu−Fe	1	2.57	0.0082	[−2.98]		

[a] Group is the chemical unit defined for the multiple scattering calculation. N_s is the number of scatterers (or groups) per metal. R_{as} is the metal−scatterer distance. σ_{as}^2 is the mean-square deviation in R_{as}. ΔE_0 is the shift in E_0 for the theoretical scattering. [b] Numbers in square brackets were constrained either to be a multiple of the above value (σ_{as}^2) or to maintain a constant difference from the above value (R_{as} and ΔE_0). [c] f' is a normalized error (χ^2); $f' = \{\Sigma_i[k^3(\chi_i^{obs} - \chi_i^{calc})]^2/N\}^{1/2}/[(k^3\chi^{obs})_{max} - (k^3\chi^{obs})_{min}]$. [d] BVS = Ss. $s = \exp[(r_0 - r)/B]$, where $B = 0.37$, r_0[Cu(II)−N] = 1.769, and $r0$[Cu(I)−N] = 1.595 (*31*).

and is thought to be a "resting" form of the oxidase, not the oxidized state expected during catalytic turnover. The XAS data presented here for the cytochrome bo_3 quinol oxidase suggest that there is a second O or N atom about 2.5 Å from Cu_B. This could be interpreted to be consistent with the proposed peroxide adduct of the bovine oxidase. However, it is also consistent with hydroxide being ligated to Cu_B and a noncoordinated water molecule located about 2.5 Å from Cu_B. This water molecule could be a weak axial ligand to the heme Fe (sixth ligand), depending on whether the heme Fe is in-plane or out-of-plane with respect to the porphyrin ring. This is reasonable assuming that the distance between the heme Fe and Cu_B is about 4.5 Å, as it is in the *Paracoccus* cytochrome *c* oxidase. A somewhat longer distance (4.9 Å) is reported for the oxidized bovine cytochrome *c* oxidase. Quantum mechanical calculations (T. Martinez, personal communication) of the heme−copper center and surrounding protein are consistent with this (i.e., water as a weak heme Fe axial ligand) as a stable structure. Since there is no indication of a peroxide present in the fully oxidized cytochrome bo_3, we favor the interpretation that in this quinol oxidase, the oxidized Cu_B is four-coordinate (three His and OH^-) with a water in the proximal binding pocket associated with the heme o_3 Fe and about 2.5 Å from Cu_B.

The Cu XAS of cytochrome bo_3 clearly shows that the coordination number of Cu_B goes from 4 to 3 upon reduction of the enzyme by ascorbate/PMS. The data suggest the loss of one of the three histidine imidazole ligands that are observed with the oxidized enzyme. It is conceivable that this change in coordination may not apply to the entire population, and there could be a mixture of forms present. However, the data indicate that in a major fraction of the population one of the histidine imidazoles has moved away from Cu_B upon reduction of the enzyme. The data also show a strong feature indicating either an Fe or two O or N atoms located about 2.5 Å from Cu_B. It is not chemically reasonable to suppose that the heme Fe is located so close to Cu_B in the reduced quinol oxidase. None of the structural data from the homologous cytochrome *c* oxidases suggest that this is feasible. On the other hand, it can be proposed that one of the histidine imidazoles has moved upon reduction of the quinol oxidase so that the nitrogen is 2.5 Å from Cu_B, i.e., no longer coordinated (1.93 Å) but reasonably close. This, and the noncoordinating solvent molecule in the proximal binding pocket, would account for the 2.5 Å feature observed in the EXAFS, and would be consistent with the three-coordinate Cu_B (two coordinating histidine imidazoles and one coordinating water molecule).

The significance of this coordination change at Cu_B upon reduction of the quinol oxidase is not yet clear. The 2.35 Å resolution structure of the bovine cytochrome *c* oxidase (*8*) does not show any change in the protein structure in the vicinity of Cu_B. Hence, it may be that the changes observed in the current work are peculiar to the cytochrome bo_3 quinol oxidase and may not apply generally to the heme−copper oxidases. Differences between the bovine oxidase and cytochrome bo_3 have been suggested by several studies characterizing the photolysis of the CO adducts from the fully reduced enzymes. CO recombination kinetics following photolysis of the CO from the heme Fe, for example, indicate

differences between the bovine cytochrome *c* oxidase and the *E. coli* oxidase (*33*). The dissociation rate of the transiently formed Cu_B−CO adduct is substantially slower for the *E. coli* oxidase than for the bovine cytochrome *c* oxidase (milliseconds vs microseconds). FTIR studies also suggest heterogeneity of the Cu_B−CO adduct observed in cytochrome bo_3 that is not observed with the bovine oxidase (manuscript in preparation). Photoaccoustic calorimetry also suggests some changes in the protein accompanying CO binding to Cu_B that is distinct from what is observed with the bovine oxidase (*34*).

However, the current work adds to the evidence that the coordination of Cu_B may in general depend on the oxygenation or redox status of the heme−copper oxidases. This was first indicated by the structure of the azide adduct of the four-subunit *Paracoccus* cytochrome *c* oxidase (*5*) in which only two of the expected three histidine imidazoles can be observed ligated to Cu_B. This has been explained as being due to local disorder of this one histidine side chain, since it is not tethered to Cu_B due to the presence of azide. In contrast, the azide adduct of the fully oxidized bovine cytochrome *c* oxidase has all three histidine imidazoles ligated to Cu_B, again indicating some differences among the heme−copper oxidases (*8*). Hence, the data in the current work with the cytochrome bo_3 quinol oxidase, considered along with the effect of azide on the *Paracoccus* cytochrome *c* oxidase, add credibilitiy to the suggestion that changes in the Cu_B ligation may occur during catalysis. Whether this is generally the case for the heme−copper oxidases and whether this is important for proton pumping will require further study of the catalytic intermediates.

SUPPORTING INFORMATION AVAILABLE

Curve fitting results for Cu EXAFS modeled as $Cu(imid)_x(N,O)_y(S/Cl,Fe,O)_z$. This material is available free of charge via the Internet at http://pubs.acs.org.

REFERENCES

1. Garcia-Horsman, J. A., Barquera, B., Rumbley, J., Ma, J., and Gennis, R. B. (1994) *J. Bacteriol. 176*, 5587−5600.
2. Ferguson-Miller, S., and Babcock, G. T. (1996) *Chem. Rev. 96*, 2889−2907.
3. Ostermeier, C., Iwata, S., and Michel, H. (1996) *Curr. Opin. Struct. Biol. 6*, 460−466.
4. Ostermeier, C., Harrenga, A., Ermler, U., and Michel, H. (1997) *Proc. Natl. Acad. Sci. U.S.A. 94*, 10547−10553.
5. Iwata, S., Ostermeier, C., Ludwig, B., and Michel, H. (1995) *Nature 376*, 660−669.
6. Tsukihara, T., Aoyama, H., Yamashita, E., Tomizaki, T., Yamaguchi, H., Shinzawa-Itoh, K., Nakashima, T., Yaono, R., and Yoshikawa, S. (1995) *Science 269*, 1069−1074.
7. Tsukihara, T., Aoyama, H., Yamashita, E., Takashi, T., Yamaguichi, H., Shinzawa-Itoh, K., Nakashima, R., Yaono, R., and Yoshikawa, S. (1996) *Science 272*, 1136−1144.
8. Yoshikawa, S., Shinzawa-Itoh, K., Nakashima, R., Yaono, R., Yamashita, E., Inoue, N., Yao, M., Fei, M. J., Libeu, C. P., Mizushima, T., Yamaguchi, H., Tomizaki, T., and Tsukihara, T. (1998) *Science 280*, 1723−1729.
9. Wikström, M. (1998) *Biochim. Biophys. Acta 1365*, 185−192.
10. Gennis, R. B. (1998) *Biochim. Biophys. Acta 1365*, 241−248.
11. Riistama, S., Hummer, G., Puustinen, A., Dyer, R. B., Woodruff, W. H., and Wikström, M. (1997) *FEBS Lett. 414*, 275−280.
12. Puustinen, A., Bailey, J. A., Dyer, R. B., Mecklenburg, S. L., Wikström, M., and Woodruff, W. H. (1997) *Biochemistry 36*, 13195−13200.
13. Lübben, M., and Gerwert, K. (1996) *FEBS Lett. 397*, 303−307.
14. Hellwig, P., Rost, B., Kaiser, U., Ostermeier, C., Michel, H., and Mäntele, W. (1996) *FEBS Lett. 385*, 53−57.
15. Morgan, J. E., Verkhovsky, M. I., and Wikström, M. (1994) *J. Bioenerg. Biomembr. 26*, 599−608.
16. Hofacker, I., and Schulten, K. (1998) *Proteins 30*, 100−107.
17. Fox, S., Nanthakumar, A., Wikström, M., Karlin, K. D., and Blackburn, N. J. (1996) *J. Am. Chem. Soc. 118*, 24.
18. Fann, Y. C., Ahmed, I., Blackburn, N. J., Boswell, J. S., Verkhovskaya, M. L., Hoffman, B. M., and Wikström, M. (1995) *Biochemistry 34*, 10245−10255.
19. Scott, R. A. (1985) *Methods Enzymol. 117*, 414−415.
20. Zhang, H. H., Filipponi, A., Di Cicco, A., Scott, M. J., Holm, R. H., Hedman, B., and Hodgson, K. O. (1997) *J. Am. Chem. Soc. 119*, 2470−2478.
21. Blackburn, N. J., de Vries, S., Barr, M. E., Houser, R. P., Tolman, W. B., Sanders, D., and Fee, J. A. (1997) *J. Am. Chem. Soc. 119*, 6135−6143.
22. Zhang, H. H., Filipponi, A., Di Cicco, A., Lee, S. C., Scott, M. J., Holm, R. H., Hedman, B., and Hodgson, K. O. (1996) *Inorg. Chem. 35*, 4819−4828.
23. Rumbley, J. N., Nickels, E. F., and Gennis, R. B. (1997) *Biochim. Biophys. Acta 1340*, 131−142.
24. Tsubaki, M., Mogi, T., Anraku, Y., and Hori, H. (1993) *Biochemistry 32*, 6065−6072.
25. Watmough, N. J., Katsonouri, A., Little, R. H., Osborne, J. P., Furlong-Nickels, E., Gennis, R. B., Brittain, T., and Greenwood, C. (1997) *Biochemistry 36*, 13736−13742.
26. Cheesman, M. R., Watmough, N. J., Pires, C. A., Turner, R., Brittain, T., Gennis, R. B., Greenwood, C., and Thomson, A. J. (1993) *Biochem. J. 289*, 709−718.
27. Fransson, G., and Lundberg, B. K. S. (1972) *Acta Chem. Scand. 26*, 3969−3976.
28. Rehr, J. J., de Leon, J. M., Zabinsky, S. I., and Albers, R. C. (1991) *J. Am. Chem. Soc. 113*, 5135.
29. Liu, W., and Thorp, H. H. (1993) *Inorg. Chem. 32*, 4102−4105.
30. Brown, I. D., and Altermatt, D. (1985) *Acta Crystallogr. B41*, 244−247.
31. Thorp, H. H. (1992) *Inorg. Chem. 31*, 1585−1588.
32. Kau, L.-S., Spira-Solomon, D. J., Penner-Hahn, J. E., Hodgson, K. O., and Solomon, E. I. (1987) *J. Am. Chem. Soc. 109*, 6433−6442.
33. Lemon, D. D., Calhoun, M. W., Gennis, R. B., and Woodruff, W. H. (1993) *Biochemistry 32*, 11953−11956.
34. Larsen, R. W., Osborne, J., Langley, T., and Gennis, R. B. (1998) *J. Am. Chem. Soc. 120*, 8887−8888.

BI982278Y